elektron ámbar

Original Article

Revista elektron, Vol. 9, No. 2, pp. 94-100 (2025)
https://doi.org/10.37537/rev.elektron.9.2.217.2025

Design and Modeling of Metamaterial-Based Antenna Arrays for Nanosatellite Communication Systems

Diseño y Modelado de Arreglos de Antenas basado en Metamateriales para Sistema de Comunicación de Nanosatélite

Axel Hemsy [#*α1], Juan Eduardo Ise [#2], Miguel Ángel Cabrera [#3], Mariano Fagre [#α4]

[#] *Laboratorio de Telecomunicaciones, Facultad de Ciencias Exactas y Tecnología, Universidad Nacional de Tucumán*
Av. Independencia 1800, Tucumán (4000), Argentina

[1] ahemsy@herrera.unt.edu.ar

[2] jise@herrera.unt.edu.ar

[3] mcabrera@herrera.unt.edu.ar

[4] mfagre@herrera.unt.edu.ar

[*] *Laboratorio de Dieléctricos, Facultad de Ciencias Exactas y Tecnología, Universidad Nacional de Tucumán*
Av. Independencia 1800, Tucumán (4000), Argentina

[α] *Consejo Nacional de Investigaciones Científicas y Técnicas (CONICET)*
Crisóstomo Álvarez 722, Tucumán (4000), Argentina

Recibido: 23/09/25; Aceptado: 17/11/25

***Abstract*— The design and modeling of compact–antenna arrays based on metamaterials for nanosatellite communication systems is presented. The main objective is to optimize performance at 2.45 GHz (S-Band). As a first step, a single coaxially fed antenna was designed on a Rogers RO4350B substrate (0.76 mm thick, $\varepsilon_r = 3.48$). A unit cell with Minkowski fractal geometry was incorporated into the ground plane, and two opposite corners of the patch were truncated to induce right-hand circular polarization.**

Different antenna arrays were designed in 1×2 (45 × 185 mm), 1×4 (48 × 155 mm), and 2×2 (75 × 85 mm) configurations, all with the same thickness of 0.76 mm. The feeding networks were implemented using Wilkinson power dividers. These arrays enabled an increase in gain to 5.1 dBi, 5.21 dBi, and 5.8 dBi, as well as an improvement in axial ratio, while maintaining efficiencies between 71% and 78%. The useful bandwidths obtained (VSWR < 2, S_{11} < -10 dB, axial ratio < 3 dB) were 22 MHz, 39 MHz and 27 MHz. The compact dimensions allow integration with the structure and subsystems onboard a CubeSat: the 1×2 and 2×2 arrays are compatible with a 1U format, while the 1×4 can be integrated into a 2U format.

Keywords: nanosatellite; antenna array; metamaterial.

***Resumen*— Se presenta el diseño y modelado de arreglos de antenas patch compacta basada en metamateriales, destinada a sistemas de comunicación para nanosatélites. El objetivo principal es optimizar el desempeño a una frecuencia de 2.45 GHz (Banda S). Como primer paso, se diseñó una antena individual con alimentación coaxial sobre un sustrato Rogers RO4350B (espesor de 0.76 mm, $\varepsilon_r = 3.48$). En el plano de tierra se incorporó una celda unitaria con geometría fractal tipo Minkowski, y se truncaron dos esquinas opuestas del parche para inducir polarización circular derecha.**

Se diseñaron diferentes arreglos de antenas en configuraciones 1×2 (45 × 85 mm), 1×4 (48 × 155 mm) y 2×2 (75 × 85 mm), todos con el mismo espesor de 0.76 mm. La alimentación se realizó mediante divisores de potencia tipo Wilkinson. Estos arreglos permitieron aumentar la ganancia a 5.1 dBi, 5.2 dBi y 5.8 dBi, y mejorar la relación axial, manteniendo eficiencias entre el 71% y el 78%. Los anchos de banda útiles obtenidos (ROE < 2, S_{11} < -10 dB, relación axial < 3 dB) fueron de 22 MHz, 39 MHz y 27 MHz. Las dimensiones compactas permiten su integración con la estructura y los subsistemas a bordo de un CubeSat: los arreglos 1×2 y 2×2 son compatibles con un formato de 1U, mientras que el 1×4 puede integrarse en un formato de 2U.

Palabras clave: nanosatélite; arreglo de antenas; metamaterial.

I. Introduction

The development of artificial satellites began with the launch of Sputnik I in 1957, marking the dawn of the space age. Since then, satellite technology has rapidly evolved toward smaller, more accessible platforms [1]. Over the past two decades, nanosatellites have gained significant attention due to their low cost, modular design, and rapid deployment capability in low Earth orbit [2]. However, the development of CubeSats for diverse missions must comply with strict limitations, including dimensions, mass, and the structure of the antenna deployment system. Antenna design is one of the critical factors in the construction of CubeSats, and it requires careful consideration of mission requirements [3].

Antennas based on metasurface achieve the essential performance required for a CubeSat mission without increasing the overall physical size of the final designs, making them geometrically and mechanically suitable for

CC BY NC ND

compact CubeSat configurations such as 1U and 1.5U. The metasurface patch antenna in the S, C, Ku, Ka and W-bands stand out are low-profile, small, have minimal power consumption, and do not require any deployment equipment [4, 5].

In [6] they investigated a UHF antenna for nanosatellite communication that incorporated a metamaterial-inspired *Epsilon-and-Mu-Near-Zero* (EMNZ) structure on the ground plane, combined with a meander line radiator. Their study showed that a 3×2 unit-cell metamaterial arrangement stabilized the resonance frequency against coupling with the nanosatellite metallic structure, exhibiting EMNZ characteristics between 385 MHz and 488.5 MHz. This finding is directly relevant for miniaturized arrays, as it demonstrates that integration with the metallic CubeSat body can cause resonance shifts and additional losses if not explicitly considered.

In [7] they proposed a spiral-shaped metamaterial patch antenna operating at 2.1 GHz, with a bandwidth of 35.1 MHz and a directivity of 7.4 dBi. In [8] they analyzed the influence on signal polarization when a metasurface was placed at a certain distance above a patch antenna. The designed and fabricated antenna operates at 2.49 GHz with a gain of 5.7 dB.

In [9] the benefits of using metamaterials in S-band patch antennas are highlighted. Their work compared a conventional antenna with a metamaterial-based antenna fed by a microstrip line, concluding that the inclusion of unit cells in the ground plane allowed a 21% size reduction, as well as improved efficiency and reduced axial ratio.

This work presents the design and modeling of a metamaterial-based patch antenna array operating in the S-band for nanosatellite communication systems, enabling a reduction in dimensions compared to a conventional patch antenna design, compatible with a 1U or 2U format.

II. Antenna Design Methodology

The antenna is intended to provide efficient communication between small satellites and Earth. Therefore, it must meet the specifications listed in Table I.

TABLE I
Required Performance

Parameter	Required value
S_{11}	< -10 dB
VSWR	<2
Gain	> 3 dBi
Polarization	Circular
Axial ratio	<3 dB

The work was carried out in two stages. First, a single antenna was designed and modeled, and subsequently, arrays were assembled in 1×2, 1×4, and 2×2 configurations.

A. Individual antenna

The patch antenna was designed on a Rogers RO4350B substrate, whose characteristics are summarized in Table II. A coaxial feed was selected, as it provides an easier and more reliable connection to the nanosatellite platform.

TABLE II
Rogers RO4350B Substrate

Dielectric constant	(3.48 ± 0.05)
Loss tangent	0.0031 (2.5 GHz)
Dielectric thickness	(0.76 ± 0.05) mm
Copper thickness	0.035 mm

The design consists of a square patch with two opposite corners truncated by circular cuts. In this work, right-hand circular polarization is considered. The radius of the truncated circle was optimized during simulation.

Given the constraints of nanosatellite applications, maintaining a physical gap between the metamaterial and the antenna was considered impractical, as it could trap space debris, potentially degrading performance or causing structural damage. To overcome this limitation, the metamaterial unit cell was embedded into the ground plane, thereby eliminating the need for mechanical separation and contributing to a reduction in the antenna's overall volume [9].

A unit cell was etched into the ground plane directly beneath the patch to reduce the antenna's physical dimensions [10]. The geometry corresponds to a first-iteration Minkowski fractal structure [11–13]. The unit cell was simulated using a combination of perfect electric conductor (PEC) and perfect magnetic conductor (PMC) boundaries, confirming that its resonance frequency lies within the S-band. The S11 parameter, shown in Fig. 2, indicates that the structure resonates at 2.7 GHz. Attempts to lower the resonance frequency of the metamaterial unit cell led to a degradation of the antenna radiation parameters, because the cell became larger than the patch.

Fig. 1 shows the front and back view of the individual antenna, while its dimensions are detailed in Table III.

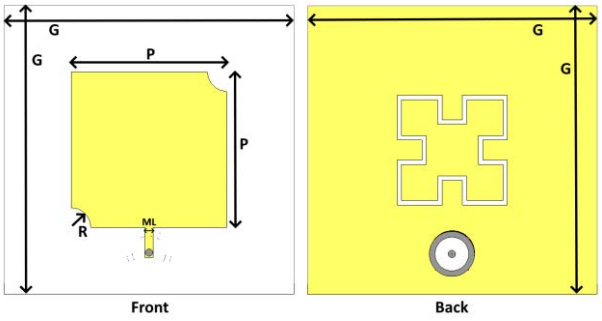

Fig. 1. Front and back view of the individual antenna.

TABLE III
Dimensions of the Individual Antenna

Parameter	Value
Ground width/length (G)	40 mm
Patch width/length (P)	21.5 mm
Truncation radius (R)	2.7 mm
Microstrip line width (ML)	1.1 mm

B. Antenna Arrays

Based on the individual antenna design, arrays were designed in three different configurations: 1×2, 1×4, and 2×2, with the objective of increasing gain and improving coverage.

Each array was assembled using a symmetric in-phase branched feeding network with Wilkinson power dividers to ensure balanced signal distribution. Quarter-wavelength (λ/4) T-junction transformers were employed for impedance matching.

Fig. 3 shows the models of the designed arrays, while the physical dimensions are presented in Table IV.

Due to their compact dimensions, the 1×2 and 2×2 arrays are compatible with a 1U nanosatellite format (10 cm cube), while the 1×4 array, due to its larger length, can be integrated into a 2U format.

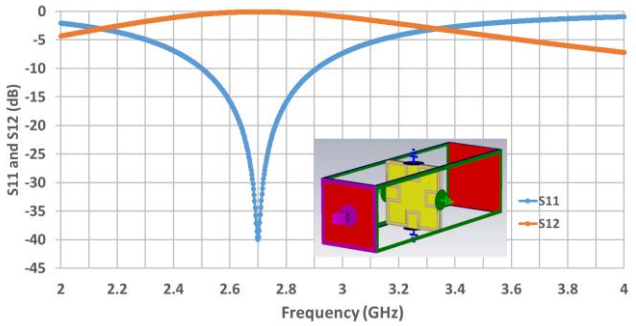

Fig. 2. Unit cell simulation. The structure resonates at 2.7 GHz.

TABLE IV
DIMENSIONS OF THE ANTENNA ARRAYS

Parameter	1x2	1x4	2x2
Ground width (GW)	45 mm	48 mm	75 mm
Ground length (GL)	85 mm	155 mm	85 mm
Patch width/ length (P)	22 mm	18 mm	21 mm
Truncation Radius (R)	2.6 mm	2.6 mm	2.3 mm
Microstrip line width (ML)	1.1 mm	1.1 mm	1.1 mm
Wilkinson divider width (W)	0.51 mm	0.51 mm	0.51 mm
Antenna spacing (Z)	20.5 mm	20.75 mm	21.5 mm

III. RESULTS AND DISCUSSION

This section presents the simulation results obtained with CST Studio Suite. The main parameters used to analyze the performance of the different proposed antenna arrays are presented below.

A. Return Loss – Parameter S_{11}

Fig. 4 and Table V show the return loss (S_{11}) results for the single antenna and the three proposed arrays.

The single antenna exhibits a resonance frequency centered at 2.442 GHz, with a return loss of –17.7 dB. The 1×2 array resonates at 2.482 GHz, achieving a return loss of –42.8 dB. The 1×4 array presents a resonance at 2.464 GHz with a return loss of –29.2 dB. In the case of the 2×2 array, two resonance peaks are observed: one at 2.422 GHz with a return loss of –38.9 dB, and another at 2.496 GHz with –26.5 dB.

The bandwidth, defined by the condition S11 < –10 dB, is summarized in Table V. Among all configurations, the 2×2 array achieves the widest bandwidth, reaching 160 MHz. The 1×2 array presents an intermediate bandwidth of 124 MHz, while the 1×4 array and the single antenna exhibit narrower responses of 90 MHz and 82.3 MHz, respectively.

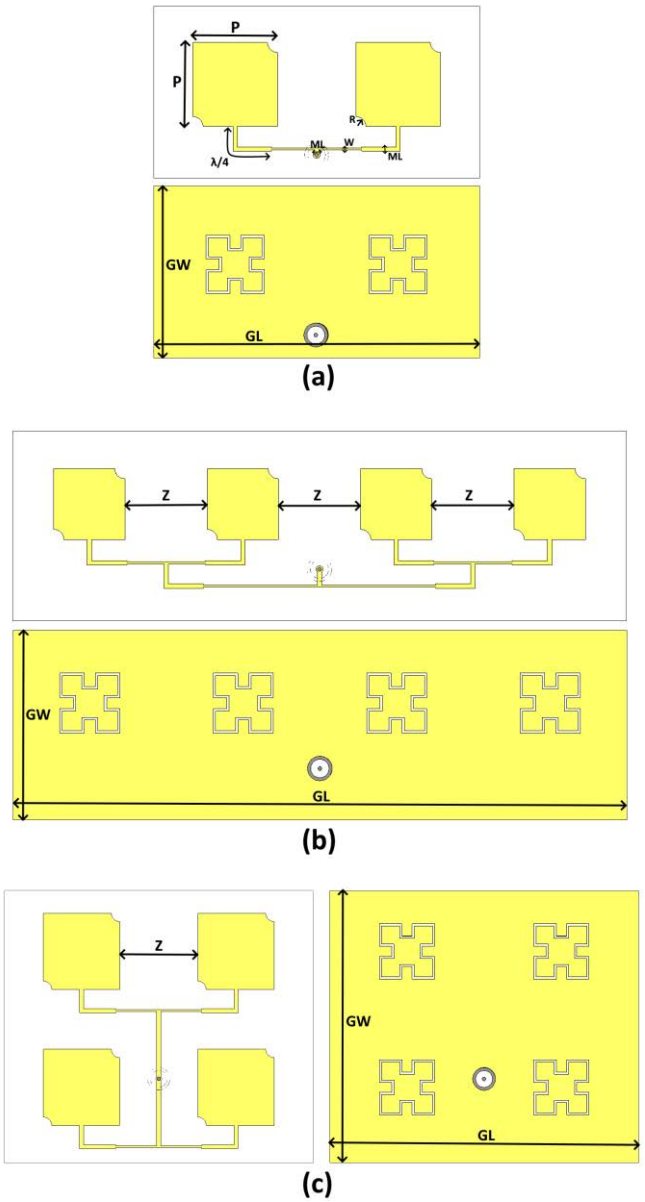

Fig. 3. Antenna arrays. Top face (white) and bottom face (yellow). (a) 1x2, (b) 1x4, (c) 2x2.

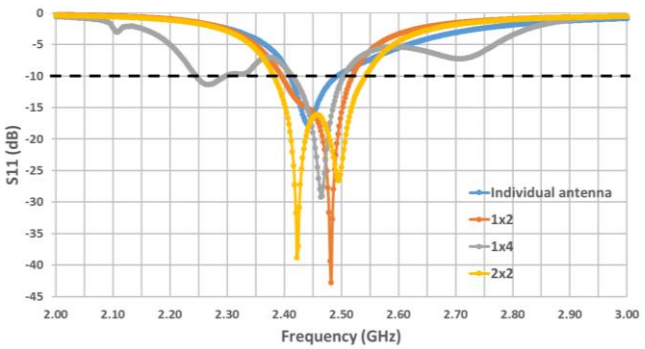

Fig. 4. S_{11} parameter as a function of frequency for the single antenna and the three arrays.

TABLE V
S_{11} PARAMETERS AND GAIN OF THE ANTENNAS

	Individual antenna	1x2	1x4	2x2
Frequency (GHz)	2.442	2.482	2.464	2.422 and 2.496
S_{11} (dB)	-17.7	-42.8	-29.2	-38.9 and -26.5
Bandwidth (S11<-10 dB)	(2.410 – 2.4923) GHz 82.3 MHz	(2.395 – 2.519) GHz 124 MHz	(2.414 – 2.504) GHz 90 MHz	(2.382 – 2.542) GHz 160 MHz
Gain at 2.45 GHz	3.6 dBi	5.1 dBi	5.2 dBi	5.8 dBi

In addition, Table V includes the gain values obtained at 2.45 GHz for each design. It can be observed that the single antenna satisfies the requirement of achieving a gain above 3 dBi, reaching 3.6 dBi. The gain increases to 5.1 dBi in the 1×2 array. For the arrays with four elements, the gain also improves: the 1×4 array achieves 5.2 dBi, and the 2×2 array reaches 5.8 dBi. The frequency-dependent behavior of the gain with right-hand circular polarization is depicted in Fig. 5.

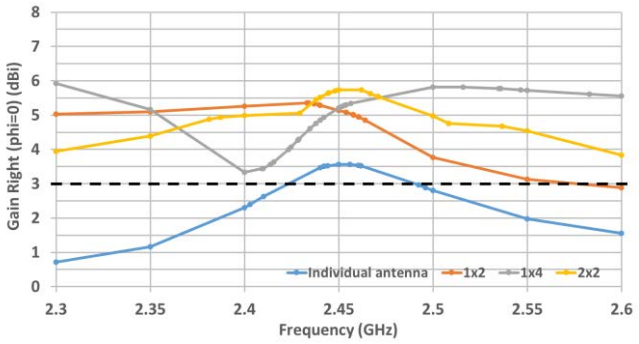

Fig. 5. Gain whit right-hand polarization as a function of frequency.

B. Voltage Standing Wave Ratio (VSWR)

Fig. 6 shows the VSWR variation as a function of frequency for the single antenna and the proposed arrays. In all cases, the minimum VSWR occurs at the operating frequency, indicating proper impedance matching between the radiating element and the feed line.

According to the results, the single antenna presents a minimum VSWR of 1.3 at 2.442 GHz. The 1×2 array achieves the lowest value of 1.02, indicating excellent impedance matching. The 1×4 array maintains good matching with a minimum of 1.07, while the 2×2 array exhibits two minima: 1.02 at 2.422 GHz and 1.1 at 2.496 GHz.

In all cases, the values remain below 2 within the operating range, fulfilling the design criteria.

C. Radiation Efficiency

Fig. 7 shows the radiation efficiency for the single antenna and the arrays. At their respective operating frequencies, the single antenna exhibits the highest efficiency of about 87%. The 1×2 array presents a reduced efficiency of around 75%, while the 1×4 array reaches approximately 78%. The 2×2 array presents the minimum efficiency, close to 71-73%.

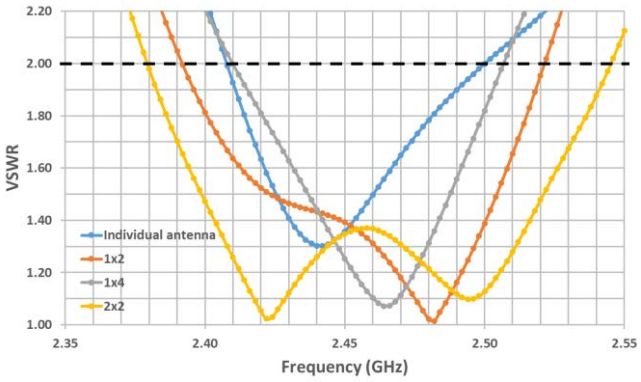

Fig. 6. VSWR as a function of frequency.

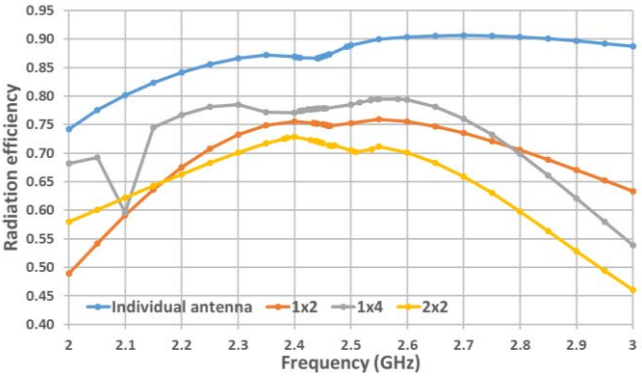

Fig. 7. Radiation efficiency as a function of frequency.

D. Axial Ratio

A perfectly circularly polarized signal has an axial ratio equal to 1 (0 dB). Fig. 8 shows the results for the axial ratio of the different configurations.

The 1×2 array achieves an axial ratio of 0.85 dB at 2.45 GHz, while the 1×4 array provides an even lower value of 0.197 dB at 2.435 GHz. The 2×2 array shows a slightly higher axial ratio of approximately 1.65 dB at 2.462 GHz. In contrast, the single antenna exhibits an axial ratio of 2.23 dB, which remains below the 3 dB limit required for circular polarization and is therefore acceptable.

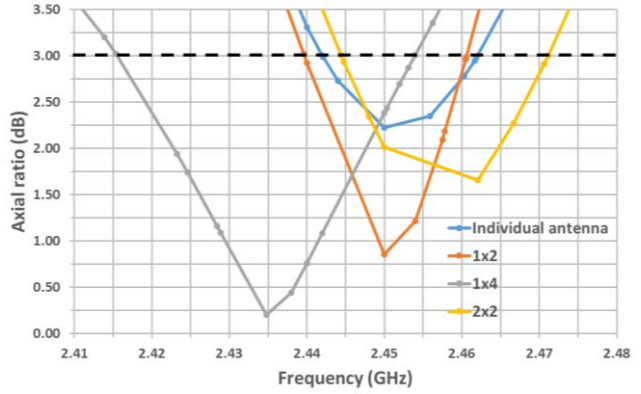

Fig. 8. Axial ratio as a function of frequency.

E. Useful Bandwidth

The useful bandwidth is defined as the frequency range that simultaneously satisfies all the technical requirements specified in Table I. For the antennas in this work, the

condition of an axial ratio below 3 dB is met alongside the other requirements.

According to the results summarized in Table VI, the individual antenna provides a useful bandwidth of 20 MHz. The 1×2 array shows a slightly improved bandwidth of 22 MHz, while the 1×4 array achieves the widest range at 39 MHz, representing a significant enhancement in operational bandwidth. The 2×2 array offers a useful bandwidth of 27 MHz, also outperforming the single antenna configuration.

TABLE VI
USEFUL BANDWIDTH

Array	Useful bandwidth
Individual antenna	(2.442 - 2.462) GHz 20 MHz
1x2	(2.439 - 2.461) GHz 22 MHz
1x4	(2.415 – 2.454) GHz 39 MHz
2x2	(2.444 – 2.471) GHz 27 MHz

F. Radiation Pattern

Fig. 9 shows the far-field radiation patterns for the four configurations under study. The single antenna exhibits a half-power beamwidth (HPBW) of 97°. For the 1×2 array, the HPBW is reduced to 66.6°, while in the 1×4 array it decreases more sharply to 34.4°, evidencing the expected directivity enhancement as the number of radiating elements increases. The 2×2 array presents a HPBW of 68°, which is consistent with its balanced distribution of radiating elements.

In all cases, the direction of maximum radiation remains close to broadside, with no significant deviations. This confirms that the proposed array configurations preserve the desired radiation orientation while improving directivity and narrowing the beamwidth.

A recent study [12] analyzed a Minkowski fractal antenna with complementary split ring resonators (CSRRs) embedded in a modified ground plane. The authors reported substantial improvements in both bandwidth and gain: maximum measured gain reached approximately 5.2 dB, and both simulated and experimental results confirmed more than 2 GHz of operating bandwidth. These findings highlight that fractal geometries combined with CSRR structures can effectively enhance bandwidth without losing consistency between simulation and measurement.

G. Surface Currents

Fig. 10 shows the surface current distribution for the 2×2 array. As observed, the highest intensity is concentrated along the edges of the radiating patches, a typical behavior due to edge effects, where charge accumulation is greater.

On the ground plane, the highest current density is located around the unit cells. This introduced fractal design modifies the electromagnetic response of the system, contributing both to the frequency shift of the antenna resonance and to the generation of circular polarization [9].

The corresponding plots for the other configurations are not included, as they exhibit qualitatively similar current distributions.

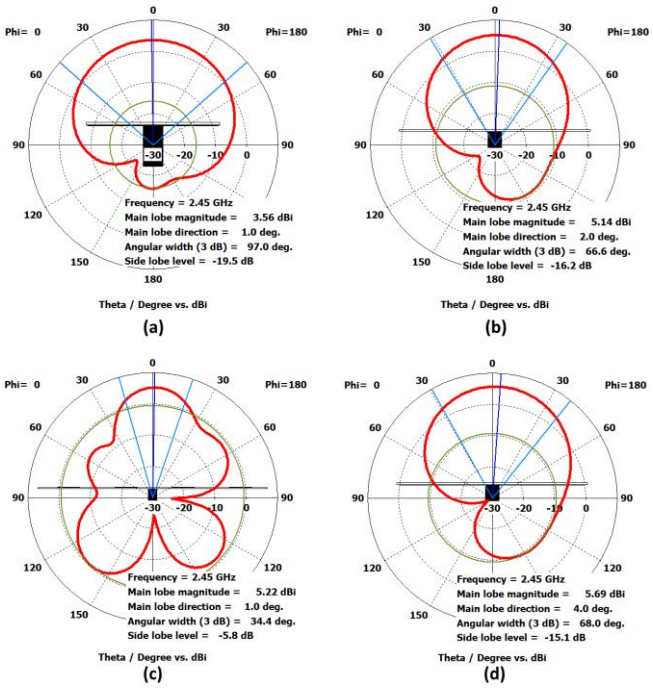

Fig. 9. Farfield gain with right-hand circular polarization (φ = 0°). (a) Single antenna. (b) 1×2 array. (c) 1×4 array. (d) 2×2 array.

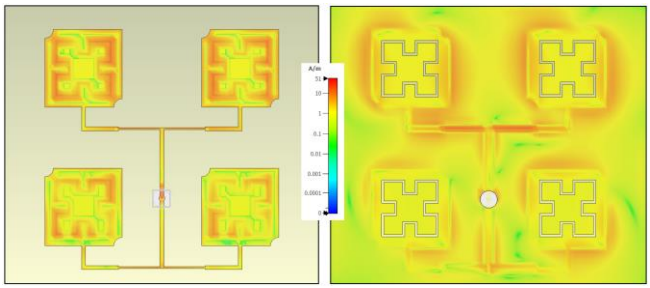

Fig. 10. Surface currents in the 2×2 array, top and bottom view.

H. Comparison with Literature

The incorporation of a unit cell in the ground planes of the designed antennas allowed for a reduction of the resonance frequency through the addition of series or shunt inductive and capacitive elements, leading to a decrease in the electrical size of the structure.

The results obtained in this work were compared with those reported in previous publications and commercial datasheets. It should be noted that no references of metamaterial-based arrays were found to enable a direct comparison.

Table VII presents a comparison of 1×4 configurations. The design proposed in this work shows a significantly smaller volume compared to the arrays developed by [14] and [15]. Although the obtained gain is somewhat lower, the axial ratio is considerably smaller, indicating purer circular polarization.

Table VIII compares the proposed 2×2 array with commercial antenna catalogs. The proposed design operates at a higher frequency (2.45 GHz), with a considerably smaller volume and an acceptable axial ratio, although with lower gain than commercial antennas.

TABLE VII
COMPARISON OF THE 1X4 ARRANGEMENT WITH THE BIBLIOGRAPHY

Reference	Frequency (GHZ)	Dimensions (mm)	Surface (cm^2)	Useful Bandwidth	Gain	Axial ratio	Gain/ surface (dBi/ cm^2)
[14]	2.25 GHz	300 x 160 (3U X 2U)	480	37.3 MHz	9.281 dBi	0.6426 dB	**0.019**
[15]	2.30 GHz	280 x 65 (2U)	182	152 MHz	10.56 dBi	1.745 dB	**0.058**
This work	**2.464 GHz**	**48 x 155 (2U)**	**74.4**	**39 MHz**	**5.2 dBi**	**0.2 dB**	**0.07**

TABLE VIII
COMPARISON OF THE 2X2 ARRANGEMENT WITH THE BIBLIOGRAPHY

Reference	Frequency (GHZ)	Dimensions (mm)	Surface (cm^2)	Useful Bandwidth	Gain	Axial ratio	Gain/ surface (dBi/ cm^2)
[16]	1.98 – 2.20	170 x 170 (2U X 2U)	289	NA	9 dBi	0.5 dB	**0.031**
[17]	2.220	160 x 160 (2U X 2U)	256	50 MHz	11.5 dBi	NA	**0.045**
[18]	2.200 – 2.290	172.7 x 172.7 (2U X 2U)	298.3	90 MHz	11 dBic	2 dB	**0.038**
This work	**2.422 and 2.496**	**75 x 85 (1U)**	**63.7**	**27 MHz**	**5.8 dBi**	**1.65 dB**	**0.091**

Additionally, Tables VII and VIII report the gain-to-surface ratio. This metric highlights that the proposed antennas provide the highest gain per unit area among the compared designs. For instance, the 1×4 configuration of this work reaches a ratio of 0.07 dBi/cm², surpassing the designs of [14] and [15]. Similarly, the proposed 2×2 array presents a ratio of 0.091 dBi/cm², more than doubling the values reported for commercial antennas. This underlines the trade-off between miniaturization and performance, which is a critical aspect in nanosatellite antenna design due to the stringent constraints in available size.

An additional observation arising from the review of the literature is that none of the 2×2 array designs reported in commercial catalogs are compatible with the geometric constraints of a 1U nanosatellite. As shown in Table VIII, all referenced antennas require surfaces on the order of 160 x 160 mm or larger, corresponding to 2U x 2U (≈4U) configurations, making their integration unfeasible for 1U platforms. In contrast, the 2 x 2 array proposed in this work fits entirely within a 1U footprint (75 x 85 mm), representing a significant advancement toward compact circularly polarized arrays suitable for CubeSat-class spacecraft with strict size limitations.

No references were found in the literature regarding 1×2 arrays with circular polarization operating near 2.45 GHz.

The literature consistently emphasizes that miniaturization through fractal or metamaterial structures involves a trade-off: while it reduces physical size and can improve properties such as circular polarization or resonance stability, efficiency or gain often suffers. For instance, in [6] it was showed that the metamaterial array enhanced resonance stability and efficiency when integrated with the nanosatellite metallic structure, but the absolute bandwidth achieved was only ~14.9 MHz in the UHF band. This illustrates the practical performance limitations when miniaturization and robustness for space environments are simultaneously required.

IV. CONCLUSIONS

In this work, different configurations of microstrip antenna arrays were designed and analyzed with the incorporation of metamaterial-inspired unit cells etched on the ground plane. The results obtained highlight the following points:

- Effective miniaturization: The inclusion of the unit cell allowed the resonance frequency to be reduced without increasing the physical size of the antenna, achieving a significantly smaller volume compared to designs reported in the literature and commercial antennas.

- Improved circular polarization: All array configurations achieved axial ratios below 3 dB in the 2.45 GHz band, fulfilling the requirements for satellite communications. The arrays exhibited substantially lower axial ratio values than the single-element antenna, confirming the contribution of the unit-cell structure to circular polarization generation.

- Trade-off between gain and size: Although the gain of the proposed arrays is lower than that reported for certain commercial designs, the achieved balance between miniaturization, acceptable axial ratio, and reduced volume positions them as a viable alternative for space-constrained platforms such as nanosatellites.

- Surface current distribution: The current analysis showed intensity concentration along the edges of the radiating patches and around the unit cells in the ground plane. This behavior confirms the role of the fractal design in modifying the electromagnetic response of the system.

In summary, the results demonstrate that the use of metamaterial-based antenna arrays is an efficient technique for the design of miniaturized antennas with circular polarization, suitable for low-cost, small-sized space communication applications. Considering the results of the simulations shown in Table IX, it can be seen that the 2×2 array offers the highest useful bandwidth and gain while fitting within the footprint of a 1U CubeSat. Therefore, the next step of this work is to fabricate a prototype of the antenna and carry out measurements to experimentally validate the simulation results.

To strengthen the proposed design, it would be beneficial to follow the approach of [12], who fabricated physical prototypes of fractal antennas with CSRRs and demonstrated good agreement between simulated and measured results. Accordingly, fabricating at least a single-element antenna or a module of the proposed array would allow anechoic chamber measurements of real gain,

efficiency, and axial ratio, as well as an evaluation of frequency shifts due to fabrication tolerances or mechanical integration. Moreover, carrying out sensitivity analyses with ±5% variations in dielectric constant or substrate thickness could help anticipate impedance mismatches or bandwidth degradation in practical CubeSat implementations.

TABLE IX
PERFORMANCE COMPARISON AT 2.45 GHZ

	1x2	1x4	2x2
Useful bandwidth	22 MHz	39 MHz	27 MHz
Gain	5.1 dBi	5.2 dBi	5.8 dBi
Size	45 x 85 x 0.76 mm	48 x 155 x 0.76 mm	75 x 85 x 0.76 mm

REFERENCES

[1] B. Peraza-Acosta, J. I. Grageda-Arellano, C. Couder-Castañeda, J. Meléndez-Martinez, D. A. Padilla-Pérez, and A. Solis-Santome, "Design and manufacture of CubeSat-type nanosatellite thermal subsystem", Scientific Reports, vol. 15, 3695, January 2025. https://doi.org/10.1038/s41598-025-86688-3

[2] S. Abulgasem, F. Tubbal, R. Raad, P. I. Theoharis, S. Lu, and S. Iranmanesh, "Antenna Designs for CubeSats: A Review", IEEE Access, vol. 9, pp. 45289-45324, March 2021. https://doi.org/10.1109/ACCESS.2021.3066632

[3] M. R. Ghaderi, and N. Amiri, "CubeSat Antenna Designs in the Last 2 Decades (2002–2023): A Survey", International Journal of Aeronautical and Space Sciences, vol. 26, pp. 327–375, January 2025. https://doi.org/10.1007/s42405-024-00800-x

[4] B. Benhmimou, F. Omari, N. Gupta, K. El Khadiri, R. A. Laamara, and M. El Bakkali, "A survey on metasurface-based antennas for CubeSat spacecrafts", Majlesi Journal of Electrical Engineering (MJEE), vol. 19(2), pp. 192542 (1-17), June 2025. https://doi.org/10.57647/j.mjee.2025.1902.42

[5] A. K. Singh, M. P. Abegaonkar, and S. K. Koul. (2022). Metamaterials for Antenna Applications. CRC Press Taylor & Francis Group. https://doi.org/10.1201/9781003045885

[6] T. Alam, M. T. Islam, and M. Cho. "Near-zero metamaterial inspired UHF antenna for nanosatellite communication system", Scientific Reports, vol. 9, 3441, March 2019. https://doi.org/10.1038/s41598-019-40207-3

[7] R. K. Prajapati, V. S. Jadaun, D. Patidar, and H. K. Gupta, "Improvement in Parameters of Patch Antenna by Using "Spiral Shapes" Metamaterial Structure", in National Conference on Recent Trends on Microwave Techniques and Application (Microwave 2012), 2012.

[8] J. L. da Silva Paiva, J. P. da Silva, A. L. Pereira de Siqueira Campos, and H. D. de Andrade, "Using metasurface structures as signal polarisers in microstrip antennas", IET Microwaves, Antennas & Propagation, vol. 13(1), pp. 23-27, January 2019. https://doi.org/10.1049/iet-map.2018.5112

[9] A. Hemsy, J. E. Ise, M. A. Cabrera, J. Scandaliaris, and M. Fagre, "Metamaterial S-band Patch Antenna Design and Modeling for Nanosatellite Communications" in 1st International Conference on Radio Frequency Communication and Networks (RFCoN), IEEE Xplore, 2025, pp. 1-6. https://doi.org/10.1109/RFCoN62306.2025.11085349

[10] M. Mirazur Rahman, Y. Yang, and S. Dey, "Application of Metamaterials in Antennas for Gain Improvement: A Study on Integration Techniques and Performance", IEEE Access, vol. 13, pp. 49489-49503, March 2025. https://doi.org/10.1109/ACCESS.2025.3552023

[11] S. Sankaralingam, S. Dhar, A. K. Bag, A. Kundu, and B. Gupta, "Use of Minkowski Fractal Geometry for the Design of Wearable Fully Fabric Compact Antenna", Journal of Physical Sciences, vol. 18, pp. 7-13, March 2014.

[12] M. A. R. Ohi, Z. Hasan, S. F. B. Faruquee, A. A. M. Kawsar, and A. Ahmed, "Wideband Minkowski fractal antenna using complementary split ring resonator in modified ground plane for 5G wireless communications", Engineering Reports, vol. 3(9), e12388, September 2021. https://doi.org/10.1002/eng2.12388

[13] A. Hemsy, J. E. Ise, F. A. Miranda Bonomi, M. A. Cabrera, and M. Fagre, "Miniaturization with Metamaterial of a Triple Band PIFA Antenna for Wi-Fi Communication", Revista Elektron, vol. 8(2), pp. 77-81, December 2024. https://doi.org/10.37537/rev.elektron.8.2.192.2024

[14] M. Darsono, and E. Wijaya, "Circularly Polarized Proximity-Fed Microstrip Array Antenna for Micro Satellite", TELKOMNIKA, vol. 11(4), pp. 803-810, December 2013. http://doi.org/10.12928/telkomnika.v11i4.1204

[15] S. Alam, E. Wijanto, B. Harsono, F. Samandatu, M. Upa, and I. Surjati, "Design of Array and Circular Polarization Microstrip Antenna for LTE Communication", in MATEC Web Conf.: The 1st International Conference on Industrial, Electrical and Electronics (ICIEE 2018), 2018, paper 03006, p. 1-8. https://doi.org/10.1051/matecconf/201821803006

[16] Commercial Antenna TechApp Consultants Ltd. Datasheet available in https://www.techappconsultants.com/copy-2-of-satraka-antenna-1

[17] Commercial Antenna IQ spacecom. Datasheet available in https://www.iq-spacecom.com/products/antennas#s-band_high_gain

[18] Commercial Antenna PlaneWave Inc. Datasheet available in https://planewaveinc.com/products/antennas/space-antennas/pw2222-101-s-band-rhcp-tx-2x2-antenna/